Analyst

COMMUNICATION

View Article Online
View Journal | View Issue

Cite this: *Analyst*, 2014, **139**, 2668

Received 25th February 2014
Accepted 28th March 2014

DOI: 10.1039/c4an00390j

www.rsc.org/analyst

Visualizing mass transport in desorption electrospray ionization using time-of-flight secondary ion mass spectrometry†

Shin Muramoto,* Thomas P. Forbes, Matthew E. Staymates and Greg Gillen

Time-of-flight secondary ion mass spectrometry (ToF-SIMS) was used to determine the effect of ambient probe incidence angle on the amount and direction of analyte molecules transported from the sample surface for desorption electrospray ionization (DESI). Incidence angle was critical to both the lateral dispersion and vertical take-off angles of analyte molecules desorbed from the surface; as the incidence angle was increased from 30° to 45° to 60° (relative to the sample surface), the lateral dispersion angle decreased from 79° to 71° to 62°, respectively, while the vertical take-off angle decreased dramatically from 12° to 6° to 4°, respectively. As for the amount of material transported, the ToF-SIMS normalized secondary ion intensity of the molecular ion (peak counts per total spectrum counts) showed a significant decrease in the signal when the incidence angle was made steeper, decreasing from 8.1×10^{-3} to 4.2×10^{-3} to 7.5×10^{-4}, respectively. The ambient mass spectrometer interfaced with DESI also showed a similar analyte response, where the intensity of the molecular ion decreased from 1.6×10^{7} counts to 3.3×10^{6} counts to 5.4×10^{5} counts, respectively. Overall, a steeper incidence angle was characterized by smaller amount of material desorption and tighter dispersion in both lateral and vertical directions. The study showed how ToF-SIMS can be used as a unique tool for characterizing the transport of desorbed analyte molecules in ambient ionization mass spectrometry, potentially offering new interface designs for optimal analyte collection.

Introduction

With the development of desorption electrospray ionization (DESI) for ambient surface mass spectrometry,[1,2] there has been a rapid increase in the number of new ionization and desorption methods that operate in atmosphere.[3] One major attribute that contributed to the expansion of ambient ionization techniques was the ability to directly analyze samples in their native environment with minimal sample preparation, in comparison to more traditional surface chemical analytical techniques such as secondary ion mass spectrometry (SIMS) that requires analysis to take place inside a vacuum. Other attributes such as low cost, portability, and fast-throughput have undoubtedly helped expand ambient techniques to a wide range of application areas. However, the technique's repeatability is associated with a large degree of uncertainty, highlighted by literature indicating the need to configure instrument geometry, type of analyte, substrate, spray solution chemistry, and even the type of mass analyzer in order to obtain repeatable measurements.[1,4–6] This has been further emphasized by a recent inter-laboratory study of repeatability in DESI sponsored by VAMAS (Versailles Project in Advanced Materials and Standards).[7]

DESI is a droplet-based ionization source that utilizes pneumatically-assisted nebulization to emit charged solvent droplets that impinge the analyte surface.[8–12] The impinging droplets induce solvation and desorption of the surface analyte into a thin liquid film.[8,11] The transfer of momentum from the high velocity primary droplets and gas stream enable the generation of analyte containing secondary droplets. These secondary droplets are expelled toward the MS inlet and experience droplet evaporation and ionization mechanisms similar to conventional electrospray ionization through a charge residue mechanism[13] or ion evaporation.[14] A number of studies have investigated and characterized various physical aspects of DESI and other droplet-based ion sources, including spray plume and spot size,[15–17] charge transmission,[18,19] primary and secondary droplet dynamics,[12] and computational fluid dynamics (CFD) simulations of secondary droplet formation.[20,21] However, the knowledge of the transport of desorbed analyte molecules into the MS interface, with respect to how it can improve the reproducibility of the technique, is still relatively limited.

In this manuscript, time-of-flight secondary ion mass spectrometry (ToF-SIMS) was used to elucidate this process by directly imaging the spatial distribution of analyte molecules desorbed by DESI that were subsequently deposited on collector

National Institute of Standards and Technology, Gaithersburg, MD 20899, USA. E-mail: shinichiro.muramoto@nist.gov; Fax: +1-301-417-1321; Tel: +1-301-975-5997

† Electronic supplementary information (ESI) available. See DOI: 10.1039/c4an00390j

surfaces. We investigated the effect of ambient ionization source incidence angle on the relative amount and the spatial distribution of desorbed analyte molecules on the collectors. The ultimate goal is to use ToF-SIMS to provide valuable desorption profile data that can be used to improve ambient MS interface designs for optimal collection of analyte molecules.

Experiment

Sample preparation

Cocaine hydrochloride dissolved in acetonitrile at a concentration of 1 mg mL^{-1} concentration was purchased from Restek* (Bellefonte, PA) and further diluted down to 100 μg mL^{-1}. Aliquots of 1 μL each of the diluted cocaine solution were deposited onto 3 mm diameter polytetrafluoroethylene (PTFE, Teflon®) hydrophobic wells of a standard Prosolia Omni Slide™ (purchased through Prosolia, Inc., but manufactured by Cel-Line, Portsmouth, NH). The sample solution solvent was allowed to evaporate in ambient conditions prior to analysis.

Ambient pressure ionization source

The droplet-based DESI source consisted of a Prosolia Omni Spray® ion source (Prosolia, Indianapolis, IN) with a solution composition and instrument configuration described in detail elsewhere.[22] Briefly, a 1 : 1 methanol–water solution (Chromasolv® Sigma Aldrich, St. Louis, MO) in a Hamilton (Reno, NV) 1 mL gastight syringe was delivered at a flow rate of 5 μL min^{-1} using a liquid infusion syringe pump (Legato 100, KD Scientific, Holliston, MA). The source was directed toward the surface using a droplet charging potential of +4 kV at incidence angles of 30°, 45°, and 60° (±2°) with respect to the sample. Droplet nebulization was pneumatically-assisted with a N_2 coaxial carrier gas supplied at (552 ± 14) kPa (80 psig, roughly 370 mL min^{-1}). The impact of carrier gas pressure was not investigated at this time. Mass analysis was performed using the Applied Biosystems/MDS Sciex 4000 Qtrap mass spectrometer, with the following instrument parameters: curtain gas pressure of 69 kPa (10.0 psi), ion source gas pressure of 83 kPa (12.0 psi), interface heater temperature of 200 °C; declustering potential of +70 V; and an entrance potential of +10 V.

Time-of-flight secondary ion mass spectrometry

Two types of particle collectors were used: A 14 mm × 14 mm silicon wafer; and a 25 mm × 25 mm × 2 mm cotton grid constructed using a 200 μm diameter cotton thread (obtained at a local crafts shop) that was stitched unidirectionally with a spacing of 0.5 mm onto a plate frame constructed using an Objet30 3D printer (Stratasys, Eden Prairie, MN) (Fig. 1). 100 mm (100) silicon wafers (Virginia Semiconductors, Fredericksburg, VA) were diced into square pieces using a DAD341 dicing saw equipped with a 15 μm diamond impregnated blade (Disco Co., Tokyo, Japan), and were ultrasonicated in methylene chloride, acetone, and methanol (Sigma-Aldrich Co., St. Louis, MO) to remove organic contaminants. The cotton grid was used as purchased. The particle collecting substrates were positioned 8 mm away from the impact point to collect desorbed analytes

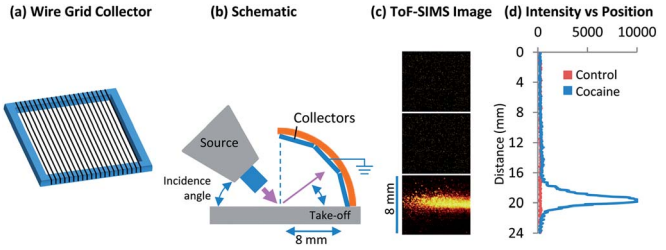

Fig. 1 (a) Diagram of the unidirectional cotton grid collector, (b) schematic representation of the experimental setup, showing the grounded silicon collectors in an array relative to the ionization source (figure not drawn to scale), (c) 2-D chemical image of the particle collectors (Si wafer) using ToF-SIMS showing the distribution of the molecular cocaine ion at *m*/*z* 304 (lighter color indicates higher intensity), and (d) cocaine intensity (counts) *versus* vertical position plot generated from the 2-D SIMS image in (c), for a control without sample and a sample with cocaine.

sputtered by the ambient ionization sources (Fig. 1). The collection substrates were analyzed using the TOFSIMS IV instrument (IONTOF GmbH, Münster, Germany) equipped with a 25 kV Bi_n^+ analysis source oriented at an incident angle of 45°. A Bi_3^+ primary ion beam in the high-current bunched mode was rastered within a 500 μm × 500 μm area to acquire a chemical image, and stitched to create large chemical images of particle collectors with a pixel density of 128 pixels per mm. For all analyses, the ion dose density was 1×10^{12} ions per cm^2. A low energy electron flood gun was used during the analysis of the cotton grid to compensate for charge build-up. The dimensions of the spread were calculated from an average of three line scans across the deposition patterns, and using 50% of the average intensity to demarcate the edges.

Schlieren imaging

A single-mirror Schlieren imaging system with a diverging light beam was used to visualize minor variances in refractive index resulting from density differences between the ambient air and flow from the ionization sources, creating an image with light and dark contrasts. The single-mirror coincident beam Schlieren system (Fig. S-2, ESI†) comprised a 41 cm diameter spherical mirror and 113 cm focal length. Images were captured using a Photron APS-RS high speed video camera (Photron USA Inc. San Diego, CA) with an acquisition frame rate of 36 frames per second.

*Certain commercial equipment, instruments, or materials are identified in this paper to adequately specify the experimental procedure. Such identification does not imply recommendation or endorsement by the National Institute of Standards and Technology, nor does it imply that the materials or equipment identified are necessarily the best available for the purpose.

Results and discussion

The current study focused exclusively on the collection of the secondary emission of analyte droplets without any external influences, therefore the potential was not applied to either the spray emitter or the MS inlet. Current measurements of the

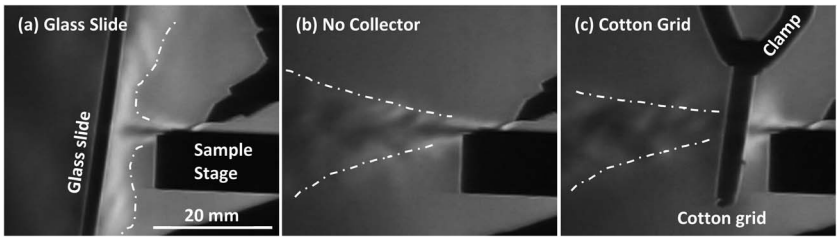

Fig. 2 Schlieren optical images of the DESI spray impacting (a) a glass microscope slide, (b) no collector, and (c) the cotton grid collector. The incidence angle of the DESI jet was 30° from the surface. Helium was used as the pneumatic-assist gas for better optical contrast. The dashed line is used to qualitatively illustrate the spreading of the jet. The substrates here were set up purely for demonstration of fluid flow, and are not representative of the setup for the particle collection experiment.

spray droplets showed that without potential applied to the spray emitter, the charge on the secondary droplets are negligible (Fig. S-1, ESI†). In addition, the collection substrates were grounded to prevent any unexpected buildup of charge, such as through contact-induced static electricity, that could affect the desorption profile through attraction or repulsion effects. After collection of analyte molecules, the collector substrates were imaged using ToF-SIMS to visualize the distribution pattern of the collected analyte. Fig. 1 shows the position of the particle collector relative to the location of the ionization probe, and ToF-SIMS images showing the distribution of the desorbed analyte molecules on the collectors.

Two collector designs were investigated to determine the effect of collector geometry on desorbed analyte distribution. The first collector, a silicon wafer, behaved similar to an impactor, where a jet impinging against a flat surface resulted in the formation of a boundary layer at the surface and a deflection of the jet's streamlines around the surface. The pneumatic-assist spray jet can be visualized by Schlieren imaging (Fig. 2), deflecting off the sample surface and impacting the collection substrate. To circumvent this flow interference at the collection surface, a unidirectional cotton grid with large spacing was used to avoid impactor issues. As displayed in the Schlieren images, the streamlines of the flowing jet appear mostly unperturbed when the cotton grid was presented in its path.

Cocaine hydrochloride displays very high ionization yield under ToF-SIMS analysis,[23] and was chosen as an ideal tracer molecule to characterize the desorption profile. Analyte was desorbed from the sample surface, and collected onto silicon wafer and cotton grid particle collectors. The DESI interrogated a 200 ng sample of cocaine for 10 s and 120 s, collected by the silicon wafer, and a 2 μg sample of cocaine for 120 s, collected by the unidirectional cotton grid. Longer exposure times were necessary for the cotton grid since the non-flat topography of the cotton thread significantly suppressed the analyte signal under ToF-SIMS analysis due to the distortion of the extraction field.[24] To quantify the analyte desorption performance, three criteria were evaluated for comparison: secondary ion intensity normalized to the total intensity (the number of ions detected at a specific peak relative to the total number of ions detected in the mass spectrum); lateral dispersion angle (calculated from the lateral spreading of analyte on the collector, *i.e.*, width); and

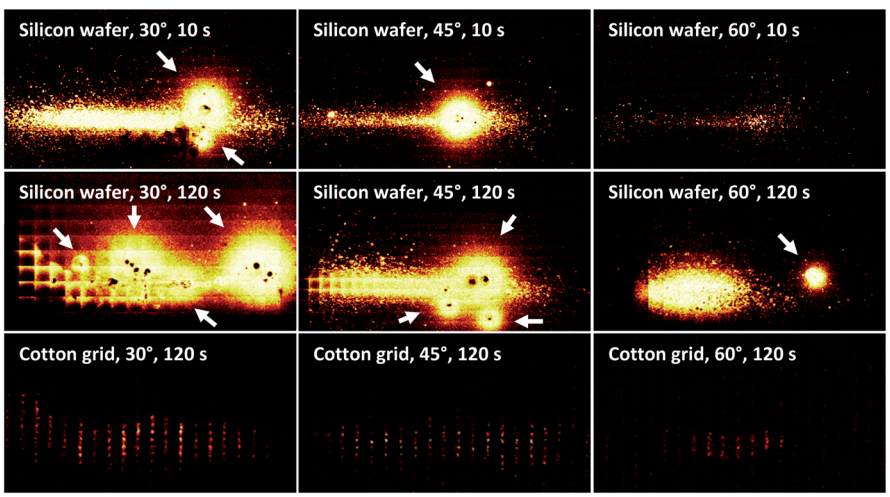

Fig. 3 ToF-SIMS chemical images of the cocaine molecule, *m/z* 304, on silicon wafer and cotton grid collectors, showing the distribution developed from DESI sampling of cocaine at 30°, 45°, and 60° from the surface. 200 ng of cocaine was sampled for 10 s and 120 s for the silicon wafer, and 2 μg was sampled for 120 s for the cotton grid. On the silicon wafers, large circles with diameters 1 mm to 3 mm (indicated by arrows) were the result of large coalesced solvent droplets transferring from the sample surface to the collector. Overall dimensions are 13 mm × 7 mm. Lighter color denotes higher intensity.

take-off angle of the analyte relative to the sample surface (calculated from the vertical spreading of analyte on the collector, *i.e.*, height).

Fig. 3 shows the ToF-SIMS chemical image of cocaine molecules desorbed by DESI. Since it was found that a majority of the desorbed analytes had low take-off angles, only the bottom collector (Fig. 1) was analyzed for all experiments. On the silicon wafer, the number of intact analyte molecules detected decreased significantly for steeper incidence angles; the normalized ion intensity of the *m/z* 304 $[M + H]^+$ peak decreased approximately an order of magnitude as the incidence angle was made steeper from 30° to 45° to 60°, decreasing from 2.1×10^{-2} to 1.8×10^{-2} to 2.7×10^{-3}, respectively. On the cotton grid, the normalized ion intensity also changed an order of magnitude from 4.7×10^{-4} to 3.1×10^{-4} to 2.3×10^{-5}, respectively. Data taken on the ambient MS system (QTrap 4000) using the same experimental conditions as the silicon wafer collector (*i.e.*, 200 ng of cocaine, Teflon coated Omni slides), showed consistent results, with an integrated intensity of 1.8×10^7 counts, 8.3×10^6 counts, and 2.2×10^5 counts at incidence angles of 30°, 45°, and 60°, respectively. Results by Takáts *et al.* support this observation that more oblique incidence angles are favored for the analysis of small molecules.[1]

One reason for increased desorption at more oblique incidence angles was most likely due to the diverging flow of the DESI spray, *i.e.*, the footprint of the impact on the surface (spot size) increased as a function of the linear distance of the probe from the impact point (probe-to-surface distance). This footprint was also affected by the angle of incidence, where spot size became a function of the cosine of the probe incidence angle. Here, the height of the DESI probe above the sample remained constant at 2 mm. Therefore, using steeper incidence angles consequently decreased the spot size, which resulted in decreased analyte desorption. Prosolia, the manufacturer of the Omni Spray ion source, has studied the relationship between spot size and probe-to-surface distance (Prosolia application note 117),[25] and observed approximately a four-fold decrease in spot size when the probe-to-surface distance was decreased from 2 mm to 1 mm. This suggested that more oblique incidence angles and greater probe-to-surface distances may be favored for increased analyte desorption.

However, a possible disadvantage of using a more oblique incidence angle was the increased lateral dispersion of the desorbed analytes. Although the increased lateral dispersion implied that a modification of inlet design could provide further enhancements in yield, the larger spot-size on the sample surface will contribute to a lower spatial resolution if the technique is used for imaging. As can be seen in Fig. 3, ToF-SIMS images of the analyte on both silicon wafers and the cotton grid showed that the spreading of the analyte occurred to a higher degree for more oblique incidence angles. For example, on the silicon wafer (10 s exposure time), incidence angles of 30°, 45°, and 60° led to a lateral spreading of 13.1 mm, 11.4 mm, and 9.6 mm, respectively (lateral dispersion angles of 79°, 71°, and 62°). The cotton grid gave very similar results, with lateral spreading of 12.9 mm, 12.1 mm, and 7.9 mm, respectively (lateral dispersion angles of 78°, 74°, 53°, respectively). Surprisingly, a longer exposure time of 120 s had not significantly increased the lateral spreading of the analyte on the silicon collector, where they remained at 14.1 mm, 11.4 mm, and 9.8 mm, respectively (Table 1).

In terms of signal reproducibility, the larger lateral spread from oblique incidence angles seemed more advantageous, as a higher density of analyte molecules spread out in a wider area would be less susceptible to experimental conditions that could affect the transport of analyte into the inlet of the MS. For example, surface imperfections or imperfections in the tip of the glass capillary could deflect the spray jet laterally. For an incidence angle of 60°, this would be troublesome since the smaller lateral dispersion requires the instrument to be set up in a, which could result in a fall in signal. In comparison, at an incidence angle of 30°, the larger dispersion angle can easily accommodate lateral deflections in the spray jet.

The vertical spreading of the analyte on the silicon wafers (10 s exposure time) were 1.7 mm, 0.9 mm, and 0.6 mm, respectively (take-off angles of 12°, 6°, and 4°, respectively), while those on the cotton grids were slightly higher at 2.1 mm, 1.6 mm, and 1.0 mm, respectively (vertical take-off angles of 15°, 11°, 7°, respectively). Since the secondary droplets are not charged without an applied potential at the spray emitter, the slightly higher vertical distributions were most likely caused by the wetting of the cotton threads by analyte-laden droplets. These take-off angles were roughly consistent with the angle that was experimentally determined to generate the highest analyte response by Costa *et al.*[20] The comparable dimensions of the desorbed analyte patterns on the silicon wafer (10 s exposure time) and the cotton grid showed that the perturbation of the DESI spray jet by the solid substrate did not lead to changes in the desorption profile. This indicated that for *short exposure times*, solid substrates can be used for particle collection because the inertia of the solvent droplets was not seen to be affected by deflected streamlines. This was advantageous since silicon wafers contribute minimal topographical, morphological, chemical, and charging effects, presenting an ideal substrate for ToF-SIMS imaging. However for *longer exposure times* on solid substrates, the transfer of coalesced solvent droplets were seen to distort the true desorption profile of the analyte. These large coalesced droplets can be seen in Fig. 3 as large circles of approximately 2 mm diameter. These droplets are the slow-moving, large coalesced droplets at the sample surface that are blown onto the collector by the pneumatic-assist gas. For the cotton grid, these droplets did not seem to present a problem as the majority of them were thought to have slipped or pushed through the grid.

The coalesced droplets present another disadvantage of using a more oblique incidence angle, as replicate analyses notably demonstrated that oblique incidence angles produced a higher frequency of coalesced droplets onto the collectors. For a DESI source interfaced to an ambient MS system, such large transfer of material may clog the MS inlet tube and lead to signal loss and even sample carryover, or they may cause detector saturation if these droplets became desolvated. The frequency and size of the transferred coalesced droplets are also expected to depend on other source and configuration

Table 1 DESI collection values of observed cocaine signal on the silicon wafer and cotton grid collectors, showing the ToF-SIMS normalized secondary ion (SI) intensity, vertical spreading (take-off angle), and lateral spreading (dispersion angle) for the three probe incidence angles. Angles in parentheses are mean angles. The large uncertainties in SI intensities are due to the random transfer of coalesced droplets (see Fig. 3)

		Silicon wafer (10 s exposure)			Cotton grid (120 s exposure)		
		SI intensity (10^{-3})	Height (mm) (angle)	Width (mm) (angle)	SI intensity (10^{-3})	Height (mm) (angle)	Width (mm) (angle)
DESI	30°	21.1 ± 5.3	1.7 ± 0.2 (12°)	13.1 ± 0.6 (79°)	0.47 ± 0.05	2.1 ± 0.2 (15°)	12.9 ± 0.5 (78°)
	45°	17.8 ± 3.1	0.9 ± 0.1 (6°)	11.4 ± 0.3 (71°)	0.31 ± 0.07	1.6 ± 0.6 (11°)	12.1 ± 1.1 (74°)
	60°	2.7 ± 0.1	0.6 ± 0.1 (4°)	9.6 ± 0.3 (62°)	0.02 ± 0.01	1.0 ± 0.2 (7°)	7.9 ± 0.3 (53°)

parameters such as solvent flow rate, solvent composition, pneumatic-assist gas pressure, sampling surface hydrophobicity, the magnitude of the potential applied to the spray emitter, and charging of the surface, however, a full investigation of these parameters was outside the scope of this study and will be pursued in future communications.

The benefit of using ToF-SIMS for imaging is its ability to detect monolayer coverage of analyte molecules on the surface. Imaging the collection substrate after a very short exposure time is similar to taking a "snapshot" photograph to visualize the instantaneous accumulation of analyte. Other imaging techniques that use fluorescent dyes and tracers require the accumulation of a relatively large amount of both analyte and tracers for imaging, both of which may diffuse out with longer exposure times and create an overestimated footprint on the particle collector. This was demonstrated in part in Fig. 3 where DESI exposure time was increased from 10 s to 120 s, where an increased frequency of solvent droplet transfers had distorted the true desorption profile of the analyte.

Conclusions

Time-of-flight secondary ion mass spectrometry (ToF-SIMS) was used to characterize the spatial distribution of desorbed analyte, demonstrating its capability to characterize fundamental desorption parameters of ambient ionization mass spectrometry. For this study, the technique was able to clearly demonstrate the effect of probe incidence angle on the desorption profile of the analyte. The desorption profiles were heavily influenced by the incidence angle of the probe, with more oblique incidence angles leading to an increased transfer of analyte onto the collector with larger dispersion angles. Most notably, longer exposure times corresponded with a higher frequency of coalesced droplets being transferred to the collector and amplifying the actual desorption footprint. This highlighted the strength of ToF-SIMS with its ability to visualize instantaneous accumulation of analyte, whereas other visualization techniques would require much longer exposure times, distorting the true desorption profile. Current work involves the investigation of other source and configuration parameters such as solvent flow rate, pneumatic-assist gas pressure, distance from impact to MS inlet, and sampling surface hydrophobicity on the amount of analyte transferred and its angle of dispersion. The knowledge of how analyte desorption changes as a function of these parameters is expected to provide better instrument configurations and interface designs for more reproducible results.

Acknowledgements

The Science and Technology Directorate of the U.S. Department of Homeland Security sponsored a portion of the production of this material under Interagency Agreement IAA HSHQDC-12-X-00024 with NIST. Research was performed in part at the NIST Center for Nanoscale Science and Technology.

References

1 Z. Takáts, J. M. Wiseman and R. G. Cooks, *J. Mass Spectrom.*, 2005, **40**, 1261–1275.
2 Z. Takáts, J. M. Wiseman, B. Gologan and R. G. Cooks, *Science*, 2004, **306**, 471–473.
3 D. J. Weston, *Analyst*, 2010, **135**, 661–668.
4 F. M. Green, P. Stokes, C. Hopley, M. P. Seah, I. S. Gilmore and G. O'Connor, *Anal. Chem.*, 2009, **81**, 2286–2293.
5 Q. Hu, N. Talaty, R. J. Noll and R. G. Cooks, *Rapid Commun. Mass Spectrom.*, 2006, **20**, 3403–3408.
6 G. Kaur-Atwal, D. J. Weston, P. S. Green, S. Crosland, P. L. R. Bonner and C. S. Creaser, *Rapid Commun. Mass Spectrom.*, 2007, **21**, 1131–1138.
7 E. Gurdak, T. Salter, S. Smith, M. Seah, I. Gilmore and F. Green, *Versailles Project on Advanced Materials and Standards*, 2013, http://www.npl.co.uk/upload/pdf/vamas-protocol.pdf.
8 I. Cotte-Rodríguez, Z. Takáts, N. Talaty, H. Chen and R. G. Cooks, *Anal. Chem.*, 2005, **77**, 6755–6764.
9 D. R. Justes, N. Talaty, I. Cotte-Rodriguez and R. G. Cooks, *Chem. Commun.*, 2007, 2142–2144.
10 S. Soparawalla, G. A. Salazar, E. Sokol, R. H. Perry and R. G. Cooks, *Analyst*, 2010, **135**, 1953–1960.
11 Z. Takáts, I. Cotte-Rodriguez, N. Talaty, H. Chen and R. G. Cooks, *Chem. Commun.*, 2005, 1950–1952.
12 A. Venter, P. E. Sojka and R. G. Cooks, *Anal. Chem.*, 2006, **78**, 8549–8555.
13 M. Dole, L. L. Mack, R. L. Hines, R. C. Mobley, L. D. Ferguson and M. B. Alice, *J. Chem. Phys.*, 1968, **49**, 2240–2249.
14 J. V. Iribarne and B. A. Thomson, *J. Chem. Phys.*, 1976, **64**, 2287–2294.
15 V. Kertesz and G. J. Van Berkel, *Rapid Commun. Mass Spectrom.*, 2008, **22**, 2639–2644.
16 S. P. Pasilis, V. Kertesz and G. J. Van Berkel, *Anal. Chem.*, 2007, **79**, 5956–5962.
17 J. M. Wiseman, D. R. Ifa, A. Venter and R. G. Cooks, *Nat. Protocols*, 2008, **3**, 517–524.

18 M. Volny, A. Venter, S. A. Smith, M. Pazzi and R. G. Cooks, *Analyst*, 2008, **133**, 525–531.
19 T. P. Forbes, T. M. Brewer and G. Gillen, *Appl. Phys. Lett.*, 2013, **102**, 214102–214104.
20 A. B. Costa and R. G. Cooks, *Chem. Commun.*, 2007, 3915–3917.
21 A. B. Costa and R. Graham Cooks, *Chem. Phys. Lett.*, 2008, **464**, 1–8.
22 C. Szakal and T. M. Brewer, *Anal. Chem.*, 2009, **81**, 5257–5266.
23 G. Gillen, C. Szakal and T. M. Brewer, *Surf. Interface Anal.*, 2011, **43**, 376–379.
24 J. L. S. Lee, I. S. Gilmore, I. W. Fletcher and M. P. Seah, *Appl. Surf. Sci.*, 2008, **255**, 1560–1563.
25 http://www.prosolia.com/resources/application-notes, 2007.